Generation of correlated Rayleigh fading channels for accurate simulationof promising wireless communication systems

Article (Unspecified)

Simulation Modelling Practice and Theory 25 (2012) 56–72

Contents lists available at SciVerse ScienceDirect

Simulation Modelling Practice and Theory

journal homepage: www.elsevier.com/locate/simpat

Generation of correlated Rayleigh fading channels for accurate simulation of promising wireless communication systems

Walid A. Al-Hussaibi, Falah H. Ali *

Communications Research Group, School of Engineering and Informatics, University of Sussex, Brighton BN19QT, United Kingdom

ARTICLE INFO

Article history:
Received 10 May 2011
Received in revised form 17 January 2012
Accepted 19 January 2012
Available online 29 March 2012

Keywords:
Correlated fading
Rayleigh channels
Diversity
Multiplexing
Capacity
Multi-antenna systems
Multicarrier systems

ABSTRACT

In this paper, a generalized method is proposed for the accurate simulation of equal/unequal power correlated Rayleigh fading channels to overcome the shortcomings of existing methods. Spatial and spectral correlations are also considered in this technique for different transmission conditions. It employs successive coloring for the inphase and quadrature components of successive signals using real correlation vector of successive signal envelopes rather than complex covariance matrix of the Gaussian signals which is utilized in conventional methods. Any number of fading signals with any desired correlations of successive envelope pairs in the interval [0, 1] can be generated with high accuracy. Moreover, factorization of the desired covariance matrix is avoided to overcome the shortcomings and high computational complexity of conventional methods. Extensive simulations of different representative scenarios demonstrate the effectiveness of the proposed technique. The simplicity and accuracy of this method will help the researchers to study and simulate the impact of fading correlation on the performance evaluation of various multi-antenna and multicarrier communication systems. Moreover, it enables the engineers for efficient design and deployment of new schemes for feasible wireless applications.

1. Introduction

To meet the increasing demands for wireless communication services such as internet and media rich applications, efficient exploitation of the limited spectral resources is required. Therefore, different promising multi-antenna and multicarrier communication schemes are considered as key techniques that can fulfil high spectral efficiency demand of fourth generation (4G) cellular wireless systems and potentially leading to gigabits communications. The most important schemes are multiple-input multiple-output (MIMO) [1–3], orthogonal frequency division multiplexing (OFDM) [4], multicarrier code-division multiple-access (MC-CDMA) [5], the hybrid combinations MIMO–OFDM [6], MIMO-CDMA [7,8], and MIMO-MC-CDMA [9]. However, it is well known that propagation channel modelling have a crucial impact on the performance evaluation of any wireless communication system such as reliability and capacity. Moreover, it is an important perquisite for design, deployment and integration of new techniques into real wireless applications. Hence, realistic channel modelling for different radio propagation conditions has attracted much attention by the research community [10–20].

Typically, in the analysis of multi-antenna and multicarrier systems, models of independent fading channels are usually assumed due to the lack of a simple procedure for generating fading signals with an arbitrary cross-correlation which tends to exaggerate the system gains. However, it is well known that channels' correlation has direct influence on the diversity,

* Corresponding author. Tel.: +44 (0)1273 678445; fax: +44 (0)1273 678399.
E-mail addresses: w.awad@sussex.ac.uk (W.A. Al-Hussaibi), f.h.ali@sussex.ac.uk (F.H. Ali).

1569-190X/$ - see front matter © 2012 Elsevier B.V. All rights reserved.
doi:10.1016/j.simpat.2012.01.009

multiplexing and capacity gains [5,21–25]. It can happen due to insufficient antenna separation at the transmit/receive ends, poor scattering environment, small coherence bandwidth of the channel or inadequate frequency separation among subcarriers [12,26,27].

Based mainly on Jakes' work [17] and for $\mathcal{N} \times \mathcal{N}$ desired covariance matrix of $\mathcal{N}$ correlated Rayleigh fading envelopes, accurate generation methods for $\mathcal{N} = 2$ have been presented by many researchers such as Ertel and Reed [28] and Beaulieu [29]. However, for $\mathcal{N} > 2$ envelopes, many algorithms have been proposed with different limitations that affects their applicability in realistic channel conditions such as Tran et al. [26], Sorooshyari and Daut [27], Natarajan et al. [30], and Beaulieu and Merani [31]. Generation of correlated fading processes that possess specified cross-correlation and auto-correlation functions is investigated in [32] using vector autoregressive stochastic model. In [33], Gaussian vector autoregressive process and inverse transform sampling techniques are utilized to generate fading processes with desired cross-correlation, auto-correlation, and heterogeneous probability density functions. The main shortcomings of the aforementioned methods are summarized as follows:

(1) The assumption of real covariance matrix in [30] leads to high restriction of use to special cases since covariance matrices are more likely to be complex in reality.
(2) The covariance matrix must be *positive definite* (i.e., positive eigenvalues) for successful factorization using Cholesky decomposition as in [31,32] or *positive semidefinite* (i.e., zero or positive eigenvalues) when eigenvalue decomposition is utilized [26].
(3) The *nonpositive semidefinite* or *unrealizable* covariance matrices produce unstable Gaussian vector autoregressive process as in [32,33] methods.
(4) High computational burden for covariance matrix factorization using Cholesky or eigenvalue decomposition methods as in [26,27,30–32].
(5) As $\mathcal{N}$ increased, the desired cross-correlation values will be limited to short interval of operation within the required accuracy tolerance as in [26,27,31–33].
(6) In [26,27,31–33] and for complex covariance matrices, generation of fading processes with high cross-correlation level such as 0.9 is not possible for $\mathcal{N} \geqslant 3$ and as $\mathcal{N}$ increased, the correlation level that can be simulated will decreased. Therefore, none of these methods can generate any number of fading processes with any desired covariance matrix.

To achieve the diversity, multiplexing, and capacity gains promised by multi-antenna systems, the total number of channels between transmit and receive antennas is more likely to be moderate to high. For example, MIMO system with $M_t = 4$ transmit antennas and $M_r = 4$ receive antennas has $\mathcal{N} = M_t M_r = 16$ channels. Furthermore, in multicarrier systems such as MC-CDMA, the total number of channels is usually high, for example, $\mathcal{N} = 256$ channels (subcarriers) are required to support 256 users. Consequently, hybrid combinations from these two systems will results in large number of fading channels. Therefore, all of the aforementioned promising communication schemes involve large number of fading channels which is difficult to be simulated using existing modelling methods.

In this paper, a generalized and straightforward technique is proposed for the accurate simulation of correlated Rayleigh fading channels in different multi-antenna and multicarrier communication systems. The main contributions of this work are highlighted as follows:

- The proposed approximation method is able to generate accurately *any* number of *equal* or *unequal* correlated Rayleigh fading signals with *any* desired correlation values of successive signal envelopes in the interval [0, 1].
- It is applicable for spatial and spectral correlations which include different parameters such as Doppler frequency shift, antenna spacing, angular spread, propagation delay spread and subcarriers frequency separation.
- The procedure involves coloring the inphase and quadrature components of successive signals using real correlation vector of successive signal envelopes rather than complex covariance matrix of the Gaussian signals. Hence, factorization of the desired covariance matrix is avoided to overcome the shortcomings and high computational complexity of conventional methods.
- The proposed technique is very flexible and efficient for simulating different scenarios of wireless communication systems such as single user MIMO (SU-MIMO), multiuser MIMO (MU-MIMO), CDMA, MC-CDMA, OFDM, MIMO–OFDM, MIMO-CDMA, and MIMO-MC-CDMA.
- The simplicity and accuracy of this method will help the research community and the industrial sector to simulate the performance of various promising wireless communication systems in realistic channel environment leading to efficient design and deployment of new schemes for feasible wireless applications.

The reminder of this paper is organized as follows: in Section 2, analysis of previous techniques for the generation of correlated Rayleigh fading channels is given. In Section 3, the proposed successive coloring technique is presented. Section 4 presents generalized algorithm for equal/unequal power correlated Rayleigh fading channels. In Section 5, complexity analysis of the generalized algorithm is given. Simulations of practical system scenarios are presented in Section 6. Finally, Section 7 concludes the paper.

The notations used in this paper are given as follows: bold-face uppercase and lowercase letters denote matrices and vectors. Plain lowercase letters stand for scalars. $\mathcal{C}^{m \times u}$ denotes complex $m \times u$ matrix while $\mathcal{R}^{m \times u}$ is for real $m \times n$ matrix. $E\{\cdot\}$

stands for the expectation value. Superscripts $[\cdot]^H$ and $[\cdot]^T$ stand for conjugate transposition and transposition, respectively. $J_0(\cdot)$ denotes the first-kind Bessel function of zero order.

2. Analysis of previous techniques on the generation of correlated Rayleigh fading channels

Conventionally, a vector of $\mathcal{N}$ complex colored signals $\mathbf{A} = [a_1, \cdots, a_{\mathcal{N}}] \in \mathcal{C}^{\mathcal{N}\times 1}$ with the desired complex covariance matrix $\mathbf{R}_{AA} = \mathrm{E}\{\mathbf{A}\mathbf{A}^H\} \in \mathcal{C}^{\mathcal{N}\times\mathcal{N}}$ is generated by the use of coloring matrix $\mathbf{L}$ and vector $\mathbf{Z} = [z_1, \cdots, z_{\mathcal{N}}] \in \mathcal{C}^{\mathcal{N}\times 1}$ of predefined signals from $\mathcal{N}$ unit power uncorrelated complex Gaussian sequences $z_1(t), \cdots, z_{\mathcal{N}}(t)$ that have Rayleigh envelopes. The sequence $z_k(t);\ k = 1, \ldots, \mathcal{N}$ with normalized auto-correlation function and zero cross-correlation can be generated using different methods such as sum of sinusoids (SoS) [19,20,35] and inverse discrete Fourier transform (IDFT) [26,34]. Cholesky decomposition is performed for the factorization of $\mathbf{R}_{AA} = \mathbf{L}\mathbf{L}^H$ and the resultant lower triangle coloring matrix $\mathbf{L}$ is used for $\mathbf{A} = \mathbf{L}\mathbf{Z}$ generation.

Since covariance matrices are more likely to be complex in reality, the assumption of real covariance matrix in [30] leads to high restriction of use to special cases such as the real transmit or receive antenna correlation matrices in multi-antenna systems [12,24]. In this case, *envelopes* and *phases* of the complex signals are correlated in contrast to complex covariance matrices which produce correlation in envelopes only. For example, envelopes and phases of three highly correlated Rayleigh fading signals are shown in Fig. 1 using the following *real* covariance matrix

$$\mathbf{R}_{AA} = \begin{bmatrix} 1 & 0.95 & 0.95 \\ 0.95 & 1 & 0.95 \\ 0.95 & 0.95 & 1 \end{bmatrix} \tag{1}$$

As can be seen from this figure, all envelopes and phases are very close to each other according to the given desired correlation matrix $\mathbf{R}_{AA}$.

For complex covariance matrices, algorithm of Beaulieu and Merani [31] is severely limited by the requirement of positive definite covariance matrix $\mathbf{R}_{AA}$ for successful factorization. Theoretically, covariance matrices are positive definite since the nonpositive definite matrices cannot represent feasible systems where the correlation between any two signal envelopes are not lying in the interval specified by the correlations of all other envelopes. However, covariance matrices formulated empirically for more than two signals can be nonpositive definite [26,27]. In this situation, the diagonal matrix of eigenvalues $\mathbf{\Lambda}$ resulting from eigenvalue decomposition $\mathbf{R}_{AA} = \mathbf{V}\mathbf{\Lambda}\mathbf{V}$ will have zero or negative values where $\mathbf{V}$ is eigenvector matrix. To overcome this shortcoming, eigenvalue decomposition is performed in [26] rather than Cholesky decomposition which requires the covariance matrix to be at least positive semidefinite. At cost of accuracy penalty, the procedure performs a replacement of negative eigenvalues in $\mathbf{\Lambda}$ by zeros to produce approximate $\widehat{\mathbf{\Lambda}}$ for coloring matrix calculation as $\mathbf{L} = \mathbf{V}\sqrt{\widehat{\mathbf{\Lambda}}}$.

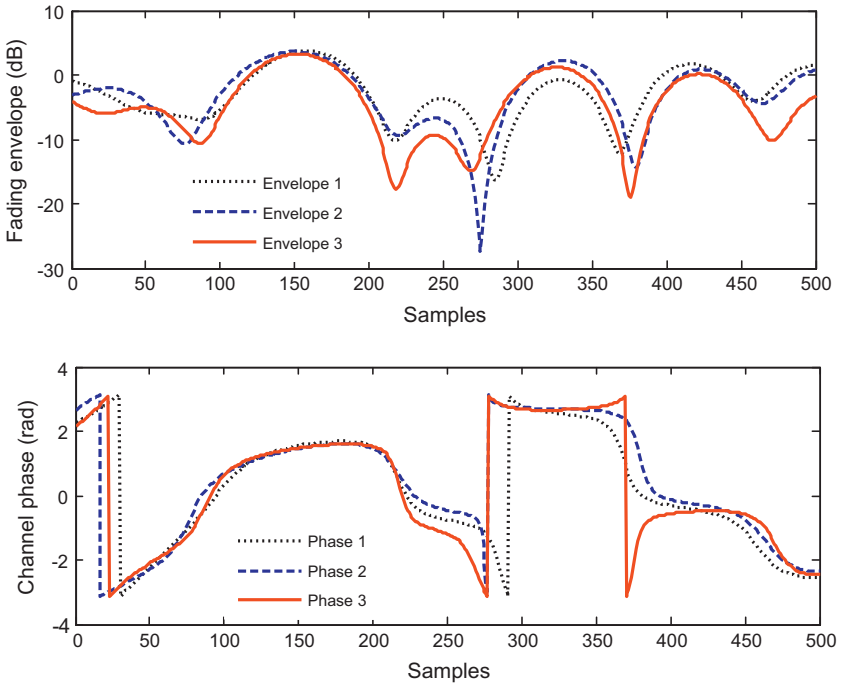

Fig. 1. Envelopes and phases of three highly correlated Rayleigh fading signals using real covariance matrix.

In [27], zero and negative eigenvalues of $\mathbf{\Lambda}$ are replaced by small positive values to find $\widehat{\mathbf{\Lambda}}$ and the approximate covariance matrix $\widehat{\mathbf{R}}_{AA} = \mathbf{V}\widehat{\mathbf{\Lambda}}\mathbf{V}$ is used for coloring matrix calculation using Cholesky decomposition as $\mathbf{L}\mathbf{L}^H = \widehat{\mathbf{R}}_{AA}$.

Complex covariance matrices of the desired correlated signals have direct influence on the performance and limitations of Tran et al. [26], Sorooshyari and Daut [27], and Beaulieu and Merani [31] algorithms. To clarify this fact by an example, Monte Carlo simulation results of probability of positive definite covariance matrices as a function of minimum correlation allowed between any pair of signal envelopes $\rho_{kq;0k\neq q};\ k,q = 1,2,\ldots,\mathcal{N}$ are illustrated in Fig. 2. Different numbers of envelopes $\mathcal{N}$ are used for different values of propagation factor $\Bbbk$ which represents the product of frequency separation between adjacent signals and the channel delay spread as will be explained in the next section. From this figure and for all $\Bbbk$ values, it is noticed that as $\mathcal{N}$ increased from 3 to 6, the probability of getting positive definite covariance matrix is decreased sharply. As a result, the algorithm of Beaulieu and Merani [31] using Cholesky decomposition can not be applied to generate $\mathcal{N} \geqslant 5$ envelopes with moderate to high correlations. This is also shown by another example where the desired correlations of all successive envelopes are set to be equal with $\Bbbk = 1$ and the range of all other correlations are measured using Monte Carlo simulation. In Table 1, cells marked by "Not valid" represent the regions where algorithm of Beaulieu and Merani [31] is not able to generate the required envelopes. Similarly, results of algorithms given in [26,27] are shown in Table 2 within error tolerance $\varepsilon = \mp 10\%$. The performance is better than of Beaulieu and Merani [31] but still unfeasible for moderate to high correlations when five or more correlated envelopes are required. As $\mathcal{N}$ increased from 3 to 6 in the examined algorithms, the range of allowed correlation between any nonsuccessive envelopes shrinks to short interval of operation within the required accuracy tolerance. Moreover, none of these algorithms is able to generate envelopes $(\mathcal{N} \geqslant 3)$ with high correlation of 0.9 and more which seriously affects the applicability of these algorithms.

3. Successive Coloring Technique (SCT)

According to the analysis of previous methods, correlation values of successive envelopes have the main influence on their performance. In the following, a simple SCT is proposed for designing any number of Rayleigh fading channels with any desired correlation level by considering real correlation vector of signal envelopes.

3.1. Principles of successive coloring

Consider a vector $\mathbf{Z}(t) \in \mathcal{C}^{1\times\mathcal{N}}$ of $\mathcal{N}$ equal power uncorrelated complex-valued i.i.d Rayleigh fading signals at time instant t as

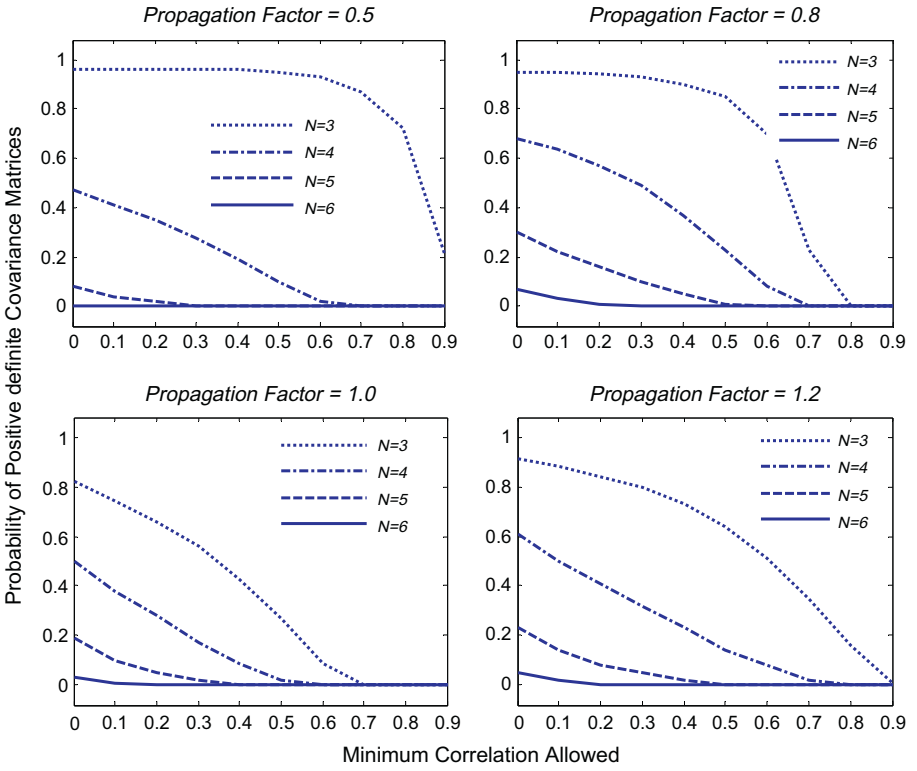

Fig. 2. Probability of positive definite covariance matrices as a function of number envelopes $\mathcal{N}$, propagation factor $\Bbbk$, and minimum correlation allowed between any pair of envelopes $\rho_{kq}, (k \neq q) = 1,\ldots,\mathcal{N}$.

Table 1
Desired correlation of all successive envelopes with $\mathbb{k} = 1$ and the range of all other correlations using algorithm of Beaulieu and Merani [31].

Desired correlation of all successive envelopes	Correlation range of all other envelopes			
	$\mathcal{N} = 3$	$\mathcal{N} = 4$	$\mathcal{N} = 5$	$\mathcal{N} = 6$
0.0	0.00–1.00	0.00–0.38	0.00–0.22	0.00–0.14
0.1	0.00–0.97	0.00–0.45	0.00–0.26	0.00–0.18
0.2	0.00–0.94	0.00–0.45	0.00–0.27	0.00–0.19
0.3	0.00–0.91	0.00–0.44	0.00–0.27	0.00–0.20
0.4	0.00–0.86	0.00–0.42	0.00–0.27	0.05–0.20
0.5	0.00–0.79	0.00–0.39	0.00–0.27	0.12–0.20
0.6	0.00–0.69	0.00–0.34	Not valid	Not valid
0.7	Not valid	Not valid	Not valid	Not valid
0.8	Not valid	Not valid	Not valid	Not valid
0.9	Not valid	Not valid	Not valid	Not valid
1.0	Not valid	Not valid	Not valid	Not valid

Table 2
Desired correlation of all successive envelopes with $\mathbb{k} = 1$ and the range of all other correlations using algorithms of Tran et al. [26] and Sorooshyari and Daut [26,27] within error tolerance $\varepsilon = \mp 10\%$.

Desired correlation of all successive envelopes	Correlation range of all other envelopes $\mp\varepsilon$.			
	$\mathcal{N} = 3$	$\mathcal{N} = 4$	$\mathcal{N} = 5$	$\mathcal{N} = 6$
0.0	0.00–1.00	0.00–0.39	0.00–0.25	0.00–0.16
0.1	0.00–1.00	0.00–0.48	0.00–0.32	0.00–0.21
0.2	0.00–1.00	0.00–0.56	0.00–0.35	0.00–0.21
0.3	0.00–1.00	0.00–0.56	0.00–0.35	0.00–0.21
0.4	0.00–1.00	0.00–0.52	0.00–0.34	0.05–0.21
0.5	0.00–0.97	0.00–0.48	0.00–0.33	0.12–0.21
0.6	0.00–0.93	0.00–0.45	0.10–0.32	Not valid
0.7	0.12–0.86	0.20–0.42	0.20–0.30	Not valid
0.8	0.40–0.84	0.25–0.35	Not valid	Not valid
0.9	Not valid	Not valid	Not valid	Not valid
1.0	Not valid	Not valid	Not valid	Not valid

$$\boldsymbol{Z}(t) = [\, z_1(t) \quad \cdots \quad z_k(t) \quad \cdots \quad z_{\mathcal{N}}(t) \,] \tag{2}$$

where

$$z_k(t) = w_k(t) + j v_k(t) \tag{3}$$

Envelope of $z_k(t)$ is $u_k(t) = |z_k(t)|$ while $w_k(t)$ and $v_k(t)$ are the in-phase and quadrature components of zero mean Gaussian random signals each with $\sigma_z^2/2$ variance. The envelope of $z_k(t)$ has Rayleigh distribution while the phase $\alpha_k(t) = \tan^{-1}(v_k(t)/w_k(t))$ is uniformly distributed over $[-\pi, \pi]$. For simplicity and notational convenience, the time index will be removed in the rest of this chapter. According to Jakes [17] and for any two uncorrelated Rayleigh fading signals z_k and z_q with $1 \leqslant (k \neq q) \leqslant \mathcal{N}$ assuming $\sigma_z^2 = 1$, the following conditions of inphase and quadrature components must be hold:

(1) $\mathrm{E}\{w_k^2\} = \mathrm{E}\{v_k^2\} = \mathrm{E}\{w_q^2\} = \mathrm{E}\{v_q^2\} = \sigma_z^2/2$.
(2) $\mathrm{E}\{w_k v_k\} = \mathrm{E}\{w_q v_q\} = 0$.
(3) $\mathrm{E}\{w_k w_q\} = \mathrm{E}\{v_k v_q\} = 0$.
(4) $\mathrm{E}\{w_k v_q\} = -\mathrm{E}\{v_k w_q\} = 0$.

The required vector $\mathbf{A} \in \mathcal{C}^{1\times\mathcal{N}}$ of $\mathcal{N}$ equal power complex-valued correlated signals having Rayleigh fading envelopes is represented by

$$\mathbf{A} = [\, a_1 \quad \cdots \quad a_k \quad \cdots \quad a_{\mathcal{N}} \,] \tag{4}$$

where $a_k = x_k + j y_k$, x_k and y_k are the in-phase and quadrature components of zero mean Gaussian random signals each with $\sigma_a^2/2$ variance. The Rayleigh distributed envelope of a_k is $r_k = |a_k|$ and the phase $\beta_k = \tan^{-1}(y_k/x_k)$ is uniformly distributed over $[-\pi, \pi]$. The inphase and quadrature components of any pair of correlated signals a_k and a_q for $1 \leqslant (k \neq q) \leqslant \mathcal{N}$ assuming $\sigma_a^2 = 1$ must satisfy the following conditions:

(1) $\mathrm{E}\{x_k^2\} = \mathrm{E}\{y_k^2\} = \mathrm{E}\{x_q^2\} = \mathrm{E}\{y_q^2\} = \sigma_a^2/2$,

(2) $\mathrm{E}\{x_k y_k\} = \mathrm{E}\{x_q y_q\} = 0$,
(3) $\mathrm{E}\{x_k x_q\} = \mathrm{E}\{y_k y_q\} = \mathscr{g}_{kq}$,
(4) $\mathrm{E}\{x_k y_q\} = -\mathrm{E}\{y_k x_q\} = \mathscr{p}_{kq}$,

where the statistics (cross-correlation parameters) $\mathscr{g}_{kq}$ and $\mathscr{p}_{kq}$ are derived for isotropic scattering assumption as a function of system specifications by Jakes [17]

$$\mathscr{g}_{kq} = \frac{J_o(2\pi f_d \tau_{kq})}{2\left(1+\mathbb{k}_{kq}^2\right)} \tag{5}$$

$$\mathscr{p}_{kq} = -\mathbb{k}_{kq} g_{kq} \tag{6}$$

where $J_0(\cdot)$ denotes the first-kind Bessel function of zero order, $f_d = vf_c/c$ is the maximum Doppler frequency, v is the mobile speed, f_c is the carrier frequency, $c = 3 \times 10^8$ m/s is the light speed, τ_{kq} is the arrival time delay between fading signals, $\mathbb{k}_{kq} = 2\pi(\Delta f_{kq})\sigma_\tau$ is the propagation factor, $\Delta f_{kq} = f_q - f_k$ is the frequency separation between signals and σ_τ is the wireless channel delay spread. Readers may refer to Jakes [17, p. 46–50] for rich details.

For desired correlated fading vector $\mathbf{A}$, the corresponding $\mathcal{N} \times \mathcal{N}$ complex covariance matrix $\mathbf{R}_{AA} = \mathrm{E}\{\mathbf{A}\mathbf{A}^H\}$ is given by

$$\mathbf{R}_{AA} = \begin{bmatrix} \gamma_{11} & \gamma_{12} & \cdots & \gamma_{1\mathcal{N}} \\ \gamma_{21}^* & \gamma_{22} & \cdots & \gamma_{2\mathcal{N}} \\ \vdots & \vdots & \ddots & \vdots \\ \gamma_{\mathcal{N}1}^* & \gamma_{\mathcal{N}2}^* & \cdots & \gamma_{\mathcal{N}\mathcal{N}} \end{bmatrix} = \begin{bmatrix} \sigma_a^2 & 2\mathscr{g}_{12} - j2\mathscr{p}_{12} & \cdots & 2\mathscr{g}_{1\mathcal{N}} - j2\mathscr{p}_{1\mathcal{N}} \\ 2\mathscr{g}_{21} + j2\mathscr{p}_{21} & \sigma_a^2 & \cdots & 2\mathscr{g}_{2\mathcal{N}} - j2\mathscr{p}_{2\mathcal{N}} \\ \vdots & \vdots & \ddots & \vdots \\ 2\mathscr{g}_{\mathcal{N}1} + j2\mathscr{p}_{\mathcal{N}1} & 2\mathscr{g}_{\mathcal{N}2} + j2\mathscr{p}_{\mathcal{N}2} & \cdots & \sigma_a^2 \end{bmatrix} \tag{7}$$

where $\gamma_{kq}, \forall(k \neq q) = 1, \ldots, \mathcal{N}$ is the cross-correlation between kth and qth complex signals (a_k and a_q) and $\gamma_{kk} =, \forall k = 1, \ldots, \mathcal{N}$ is the autocorrelation (power) of signal a_k. When $\mathbb{k}_{kq} = 0;\ k, q = 1, \ldots, \mathcal{N}$, the covariance matrix will be real and represented as

$$\mathbf{R}_{AA} = \begin{bmatrix} \sigma_a^2 & 2\mathscr{g}_{12} & \cdots & 2\mathscr{g}_{1\mathcal{N}} \\ 2\mathscr{g}_{21} & \sigma_a^2 & \cdots & 2\mathscr{g}_{2\mathcal{N}} \\ \vdots & \vdots & \ddots & \vdots \\ 2\mathscr{g}_{\mathcal{N}1} & 2\mathscr{g}_{\mathcal{N}2} & \cdots & \sigma_a^2 \end{bmatrix} \tag{8}$$

The correlation factor ρ_{kq} between the kth and qth envelopes (r_k and r_q) is given by

$$\rho_{kq} = \frac{Cov\{r_k, r_q\}}{\sqrt{Var\{r_k\}Var\{r_q\}}} = \frac{(1+\lambda_{kq})E_i[(2\sqrt{\lambda_{kq}})/(1+\lambda_{kq})] - \frac{\pi}{2}}{2 - \frac{\pi}{2}} \tag{9}$$

where $E_i[x]$ is the complete elliptic integral of the second kind with modulus x, and λ_{kq} is the magnitude of correlation between complex Gaussian signals a_k and a_q represented by

$$\lambda_{kq}^2 = \left| \frac{Cov\{a_k, a_q\}}{\sqrt{Var\{a_k\}Var\{a_q\}}} \right|^2 = \frac{\mathscr{g}_{kq}^2 + \mathscr{p}_{kq}^2}{\ell^2} \tag{10}$$

where $\ell = \sigma_a^2/2$. In [17], the correlation factor ρ_{kq} is well approximated by λ_{kq}^2 as

$$\rho_{kq} \cong \lambda_{kq}^2 = \frac{\mathscr{g}_{kq}^2 + \mathscr{p}_{kq}^2}{\ell^2} \tag{11}$$

Therefore, $\mathscr{g}_{kq}$ can be approximated as

$$\mathscr{g}_{kq} \cong \sqrt{\frac{\rho_{kq}}{1+\mathbb{k}_{kq}^2}}\,\ell \tag{12}$$

Correlation factors between any pairs of envelopes of $\mathbf{A}$ elements can be given in $\mathcal{N} \times \mathcal{N}$ correlation matrix form $\boldsymbol{\rho} \in \mathcal{R}^{\mathcal{N}\times\mathcal{N}}$ as

$$\boldsymbol{\rho} = \begin{bmatrix} \rho_{11} & \rho_{12} & \rho_{13} & \cdots & \rho_{1\mathcal{N}} \\ \rho_{21} & \rho_{22} & \rho_{23} & \cdots & \rho_{2\mathcal{N}} \\ \rho_{31} & \rho_{32} & \rho_{33} & \cdots & \rho_{3\mathcal{N}} \\ \vdots & \vdots & \vdots & \ddots & \vdots \\ \rho_{\mathcal{N}1} & \rho_{\mathcal{N}2} & \rho_{\mathcal{N}3} & \cdots & \rho_{\mathcal{N}\mathcal{N}} \end{bmatrix} \tag{13}$$

where $\rho_{kk} = 1,\ \forall k = 1,\ldots,\mathcal{N}$ is the autocorrelation of each signal envelope and $\rho_{kq} = \rho_{qk},\ \forall (k \neq q) = 1,\ldots,\mathcal{N}$. The elements of $\boldsymbol{\rho}$ are real values since they represent the correlation between envelopes (magnitudes of the complex signals).

In SCT, correlation vector $\boldsymbol{\rho}_s \in \mathcal{R}^{1\times(\mathcal{N}-1)}$ of successive pairs from ρ matrix will be considered as

$$\rho_s = \begin{bmatrix} \rho_{12} & \rho_{23} & \cdots & \rho_{(\mathcal{N}-1)\mathcal{N}} \end{bmatrix} \tag{14}$$

To generate $\mathbf{A} = [a_1\ \cdots\ a_k\ \cdots\ a_{\mathcal{N}}]$ with $a_k = x_k + jy_k$ from $\mathbf{Z} = [z_1\ \cdots\ z_k\ \cdots\ z_{\mathcal{N}}]$ with $z_k = w_k + jv_k$ assuming $\sigma_a^2 = \sigma_z^2 = 1$, the first stage of this process involves fixing $a_1 = z_1$. In the seconde stage, a_2 will be calculated by coloring z_2 with a_1 as; $a_2 = \mathcal{A}_{12}a_1 + \mathcal{B}_{12}z_2$, where $\mathcal{A}_{12}$ and $\mathcal{B}_{12}$ are *coloring factors* used to achieve the desired correlation between successive envelopes a_1 and a_2. Similarly, a_3 will be calculated in the third stage from z_3 and a_2 as; $a_3 = \mathcal{A}_{23}a_2 + \mathcal{B}_{23}z_3$, and so on. Therefore, the overall process is summarized by using the following linear formulation:

$$a_k = \begin{cases} z_k, & k = 1 \\ \mathcal{A}_{(k-1)k}a_{k-1} + \mathcal{B}_{(k-1)k}z_k, & 2 \leqslant k \leqslant N \end{cases} \tag{15}$$

where the *coloring factors*, $\mathcal{A}_{(k-1)k}$ and $\mathcal{B}_{(k-1)k}$ for $2 \leqslant k \leqslant \mathcal{N}$ are used to insure the required correlation among the inphase and quadrature components of successive envelope pairs and maintains different channel propagation conditions. For this purpose, at least one of these factors must be a complex number. Assuming that $\mathcal{A}_{(k-1)k}$ and $\mathcal{B}_{(k-1)k}$ are complex and real numbers, respectively, their values are derived directly by satisfying the aforementioned conditions of Jakes [17] in Eq. (15) and using Eqs. (6), (11), and (12) as:

$$\mathcal{A}_{(k-1)k} = \sqrt{\frac{\rho_{(k-1)k}}{1 + \mathbb{k}^2_{(k-1)k}}}[1 + j\mathbb{k}_{(k-1)k}] \tag{16}$$

$$\mathcal{B}_{(k-1)k} = \sqrt{1 - \rho_{(k-1)k}} \tag{17}$$

Correlation factors of any nonsuccessive pairs of envelopes ρ_{kq} will be in the range satisfied by the correlations of all pairs between kth and qth envelopes and determined approximately by the multiplication result of them as

$$\rho_{kq} \cong \prod_{i=k}^{q-1} \rho_{i(i+1)}; \quad k < q-1 \tag{18}$$

Note that for conventional methods, the desired correlation parameters must represent a feasible system (i.e. has a positive definite covariance matrix) in order to be simulated accurately. For example, if the desired correlations of three envelopes are $\rho_{12} = \rho_{23} = 0.9$ then as explained in [27], ρ_{13} should be in the interval [0.64, 1.0]. That is, if there is high correlation between (r_1, r_2) and (r_2, r_3), then there should be high correlation between (r_1, r_3). For this case, ρ_{13} using SCT will be 0.81 which is in the above interval. As the number of desired signals increased and/or moderate to high correlations of successive signal envelopes is required, the admissible correlation ranges of all nonsuccessive envelopes will be shrinking to the specific values of Eq. (18).

3.2. SCT algorithm

For wireless communication system, the desired channel $\mathbf{A}$ of equal power signals (σ_a^2) with an arbitrary correlation vector of successive pairs of envelopes $\boldsymbol{\rho_s}$ can be generated as follows:

1. Given the desired correlation vector $\boldsymbol{\rho_s}$ of $\rho_{(k-1)k};\ k = 1,\ldots,\mathcal{N}$ elements as in Eq. (14) and the propagation factors as $\mathbb{k}_{(k-1)k} = 2\pi(\Delta f_{(k-1)k})\sigma_\tau;\ 2 \leqslant k \leqslant \mathcal{N}$.
2. Calculate the coloring factors, $\mathcal{A}_{(k-1)k}$ and $\mathcal{B}_{(k-1)k}$ for $2 \leqslant k \leqslant \mathcal{N}$ using Eqs. (16) and (17), respectively.
3. Generate a reference vector $\mathbf{Z} = [z_1\ \cdots\ z_k\ \cdots\ z_{\mathcal{N}}]$ of $\mathcal{N}$ zero mean uncorrelated complex Gaussian signals with equal power Rayleigh envelops $(\sigma_z^2 = \sigma_a^2)$ using SoS or any other efficient method such as IDFT.
4. For $k = 1,\ldots,\mathcal{N}$, use Eq. (15) to generate the desired equal power signals of correlated Rayleigh fading channel $\mathbf{A} = [a_1\ \cdots\ a_k\ \cdots\ a_{\mathcal{N}}]$.

4. Generalized SCT (GSCT) algorithm for equal/unequal power correlated Rayleigh fading channels

As shown in the previous section, SCT to generate equal power signals is a simple procedure. However, generation of unequal power signals $\widehat{\mathbf{A}} = [\hat{a}_1\ \cdots\ \hat{a}_k\ \cdots\ \hat{a}_{\mathcal{N}}] \in \mathcal{C}^{1\times\mathcal{N}}$ is very useful for many cases such as scattered users in different distances from the base station receiver with the absence of accurate power control or unequal power transmission from the available transmit antennas. Therefore the SCT algorithm is generalized here to also generate Rayleigh fading channels for unequal signal powers with desired correlation.

Consider a desired correlation matrix $\hat{\boldsymbol{\rho}}$ of $\mathcal{N}$ signal envelopes with unequal power of $\sigma^2_{\hat{a}_k}; k = 1,\ldots,\mathcal{N}$ as;

$$\hat{\boldsymbol{\rho}} = \begin{bmatrix} \hat{\rho}_{11} & \hat{\rho}_{12} & \hat{\rho}_{13} & \cdots & \hat{\rho}_{1\mathcal{N}} \\ \hat{\rho}_{21} & \hat{\rho}_{22} & \hat{\rho}_{23} & \cdots & \hat{\rho}_{2\mathcal{N}} \\ \hat{\rho}_{31} & \hat{\rho}_{32} & \hat{\rho}_{33} & \cdots & \hat{\rho}_{3\mathcal{N}} \\ \vdots & \vdots & \vdots & \ddots & \vdots \\ \hat{\rho}_{\mathcal{N}1} & \hat{\rho}_{\mathcal{N}2} & \hat{\rho}_{\mathcal{N}3} & \cdots & \hat{\rho}_{\mathcal{N}\mathcal{N}} \end{bmatrix} \tag{19}$$

Therefore the correlation vector $\hat{\boldsymbol{\rho}}_s \in \mathcal{R}^{1\times(\mathcal{N}-1)}$ of successive pairs formulated from $\hat{\rho}$ matrix will be addressed in the generalized algorithm as

$$\hat{\boldsymbol{\rho}}_s = \begin{bmatrix} \hat{\rho}_{12} & \hat{\rho}_{23} & \cdots & \hat{\rho}_{(\mathcal{N}-1)\mathcal{N}} \end{bmatrix} \tag{20}$$

The GSCT algorithm is given below in step by step manner to describe the generation of desired signals of correlated Rayleigh fading channels for both equal and unequal powers.

1. Specify the desired powers of $\mathcal{N}$ correlated Rayleigh fading envelopes.
2. Specify the propagation factors as $\Bbbk_{(k-1)k} = 2\pi(\Delta f_{(k-1)k})\sigma_\tau;\ 2 \leqslant k \leqslant \mathcal{N}$.
3. If the desired powers of envelopes are equal (σ^2_a), specify the required correlation vector $\boldsymbol{\rho_s}$ of $\rho_{(k-1)k};\ k = 1,\ldots,\mathcal{N}$ elements as in Eq. (14) and then Go to step No. 5. Otherwise, if the desired powers of envelopes are unequal defined by $\left\{\sigma^2_{\hat{a}_k}\right\}_{k=1}^{\mathcal{N}}$, identify the correlation vector $\hat{\boldsymbol{\rho}}_s$ of $\hat{\rho}_{(k-1)k};\ k = 1,\ldots,\mathcal{N}$ elements as in Eq. (20) and continue to next step.
4. Normalize the elements of correlation vector $\hat{\boldsymbol{\rho}}_s$ to create normalized vector $\boldsymbol{\rho_s}$ using the following transformation [30]

$$\rho_{(k-1)k} = \frac{\hat{\rho}_{(k-1)k}}{\sqrt{\sigma^2_{\hat{a}_{(k-1)}}\sigma^2_{\hat{a}_k}}} \tag{21}$$

Calculate the coloring factors, $\mathcal{A}_{(k-1)k}$ and $\mathcal{B}_{(k-1)k}$ for $2 \leqslant k \leqslant \mathcal{N}$ using Eqs. (16) and (17), respectively.

5. Generate a reference vector $\mathbf{Z} = [z_1 \cdots z_k \cdots z_\mathcal{N}]$ of $\mathcal{N}$ zero mean uncorrelated complex Gaussian signals with equal power Rayleigh envelops $(\sigma^2_z = \sigma^2_a)$ using SoS [20,35] or any other efficient method such as IDFT [34].
6. For $k = 1,\ldots,\mathcal{N}$, use Eq. (15) to generate equal power signals of correlated Rayleigh fading channel represented by the vector $\mathbf{A} = [a_1 \cdots a_k \cdots a_\mathcal{N}]$. The algorithm terminates if the desired powers of all envelopes are equal, otherwise continue to the next step if they are unequal.
7. Use the transformation given in Eq. (22) similar to Natarajan et al. [30] to generate the unequal power signals represented by the channel vector $\widehat{\mathbf{A}} = [\hat{a}_1 \cdots \hat{a}_k \cdots \hat{a}_\mathcal{N}]$.

$$\hat{a}_k = \frac{\sigma_{\hat{a}_k}}{\sigma_a} a_k; \quad k = 1,\ldots,\mathcal{N} \tag{22}$$

The above algorithmic procedure is realized in MATLAB simulation environment for different practical system settings and scenarios explained in Section 6.

5. Complexity analysis of GSCT

Let's assume that $\mathcal{N}$ is the total number of desired equal power correlated signals. To simulate these signals using the desired *correlation vector* $\boldsymbol{\rho_s}$ of $\mathcal{N}-1$ conditions in GSCT, approximate computational operations of $2\mathcal{N}^2 - 3\mathcal{N} + 2$ are required which is $\mathcal{O}(\mathcal{N}^2)$ efforts. This includes additions, subtractions, divisions, multiplications, and square roots. For Cholesky and eigenvalue decomposition based methods, total calculations of $(2\mathcal{N}^3 + 3\mathcal{N}^2 + \mathcal{N})/6$ and $(6\mathcal{N}^3 - 3\mathcal{N}^2 - 3\mathcal{N})/6$ are required, respectively. Hence, the computational efforts of these methods is of $\mathcal{O}(\mathcal{N}^3)$, where the main computational burden is due the requirement of $\mathcal{N}^3/6$ multiplications for *covariance matrix* $\mathbf{R}_{AA}$ factorization. Furthermore, $\sum_{n=1}^{\mathcal{N}-1}(n)$ correlation conditions from $\mathbf{R}_{AA}$ are to be satisfied for successful generation of desired signal. Therefore, the complexity of GSCT is reduced exponentially compared with considered conventional methods. Summery of the complexity analysis is given in Table 3.

For comparison purpose, let's consider the generation of $\mathcal{N} = M_t M_r$ signals for $M_t \times M_r$ MIMO system. By using $M_t = 6$ and $M_r = 8$, the required number of signals is $\mathcal{N} = 48$. This means, 4.466×10^3 approximate calculations are needed for GSCT compared with 38.024×10^3 and 109.416×10^3 for Cholesky and eigenvalue decomposition methods, respectively. When $\mathcal{N} = 256$ such as in MC-CDMA, approximate calculations of 0.13×10^6 are required for GSCT which are significantly less than 5.62×10^6 and 16.74×10^6 for Cholesky and eigenvalue decomposition methods, respectively. Also, we find that approximately more than 100% reduction in complexity can be achieved at $\mathcal{N} = 9$ compared with Cholesky and at $\mathcal{N} = 4$ compared with eigenvalue decomposition method.

For unequal power correlated signals, GSCT requires extra $3(\mathcal{N}-1)$ calculations for $\hat{\boldsymbol{\rho}}_s$ normalization and $2\mathcal{N}$ for $\widehat{\mathbf{A}}$ elements formulation. Hence, the total extra required computations is $5\mathcal{N} - 3$. Similarly, when Cholesky or eigenvalue

Table 3
Computational complexity of GSCT to generate equal power correlated fading signals compared with the conventional methods that utilize Cholesky or eigenvalue decomposition.

Algorithm	Total calculations	Computational effort
Cholesky	$(2\mathcal{N}^3+3\mathcal{N}^2+\mathcal{N})/6$	$\mathcal{O}(\mathcal{N}^3)$
Eigenvalue	$(6\mathcal{N}^3-3\mathcal{N}^2-3\mathcal{N})/6$	$\mathcal{O}(\mathcal{N}^3)$
GSCT	$2\mathcal{N}^2-3\mathcal{N}+2$	$\mathcal{O}(\mathcal{N}^2)$

decomposition method is used, extra $3\mathcal{N}^2+2\mathcal{N}$ computations are needed. Consequently, GSCT has more significant reduction compared with the other methods.

6. Simulation results

For the accuracy checking and to demonstrate the effectiveness of GSCT without loss of generality, we consider generation of correlated Rayleigh fading signals using four different representative examples. The first example is for simulating four equal power signals of 2×2 SU-MIMO channel scenario with complex spatial covariance matrix. In the second example, we consider simulation of four equal power signals for four receive antenna correlation scenario using real spatial covariance matrix. The third example is for simulating 64 equal power signals of multi-carrier (OFDM) channel scenario with spectral correlation. The last example is for simulating unequal power signal needed in many wireless applications that experiencing spectral and/or spatial correlation such as MC-CDMA, MU-MIMO, and MIMO–OFDM. In this study, MATLAB/v.7.9 is used for the simulations. The SoS method [20] using 16 sinusoids, Doppler frequency f_d = 50 Hz, and 8 kHz sampling frequency is employed for generating the reference signal vector **Z** in all considered examples due its simplicity and accuracy. Algorithm of GSCT is applied to generate desired vector **A** of correlated signals from **Z** using the coloring factors and according to the available informations of considered examples.

Example 1. Consider generation of $\mathcal{N}=4$ equal power flat Rayleigh fading signals as $\mathbf{A}=[a_1 \quad a_2 \quad a_3 \quad a_4]$ for 2×2 SU-MIMO system scenario using $\sigma_a^2=2\ell=1$ and the following empirically formulated covariance matrix.

$$\mathbf{R}_{AA}=\begin{bmatrix} 1 & 0.58+j0.75 & 0.28+j0.37 & 0.15+j0.43 \\ 0.58-j0.75 & 1 & 0.17+j0.47 & 0.27+j0.39 \\ 0.28-j0.37 & 0.17+j0.47 & 1 & 0.58+j0.75 \\ 0.15-j0.43 & 0.27-j0.39 & 0.58-j0.75 & 1 \end{bmatrix} \tag{23}$$

The eigenvalues of $\mathbf{R}_{AA}$ are: −0.254, 0.198, 1.298, and 2.756. Since one of the eigenvalue is negative, $\mathbf{R}_{AA}$ is neither a positive semidefinite nor a positive definite matrix. Besides serving as an illustration of GSCT effectiveness, the given covariance matrix also provides an example of realistic channel conditions where the covariance matrices are not always positive definite. It should be noted that eigenvalue decomposition based method can not be used directly for this example without forcing $\mathbf{R}_{AA}$ to be positive semidefinite by replacing the negative eigenvalue with zero as in [26]. Similarly, Cholesky decomposition based method can not be employed without forcing $\mathbf{R}_{AA}$ to be positive definite by replacing the negative eigenvalue with small positive value as in [27]. However, forcing $\mathbf{R}_{AA}$ to be positive semidefinite/definite will affect its structure leading to inaccurate realistic channel simulation and hence the performance evaluation of the considered communication system.

To generate **A** using the proposed GSCT, the desired correlation matrix of envelopes ρ can be calculated directly from $\mathbf{R}_{AA}$ using Eq. (11) as

$$\rho=\begin{bmatrix} 1 & \rho_{12} & \rho_{13} & \rho_{14} \\ \rho_{21} & 1 & \rho_{23} & \rho_{24} \\ \rho_{31} & \rho_{32} & 1 & \rho_{34} \\ \rho_{41} & \rho_{42} & \rho_{43} & 1 \end{bmatrix}=\begin{bmatrix} 1 & 0.898 & 0.215 & 0.225 \\ 0.898 & 1 & 0.249 & 0.207 \\ 0.215 & 0.249 & 1 & 0.898 \\ 0.225 & 0.207 & 0.898 & 1 \end{bmatrix} \tag{24}$$

Therefore, desired correlation vector ρ_s of successive envelopes is

$$\boldsymbol{\rho_s}=[\rho_{12} \quad \rho_{23} \quad \rho_{34}]=[0.898 \quad 0.249 \quad 0.898] \tag{25}$$

Propagation factors of the successive signals are calculated also from $\mathbf{R}_{AA}$ using Eq. (6) as $\mathbb{k}_{12}=\mathbb{k}_{34}=1.29$ and $\mathbb{k}_{23}=2.76$. Envelopes (r_1, r_2, r_3, r_4) and phases (β_1, β_2, β_3, β_4) of the generated fading signals are depicted in Figs. 3 and 4, respectively. It can be seen that envelopes (r_1, r_2) and (r_3, r_4) are very close to each other which reflects the desired high correlations of $\rho_{12}=\rho_{34}=0.898$ while envelopes (r_1, r_3), (r_1, r_4), (r_2, r_3), and (r_2, r_4) are unrelated to each other due to their low correlation values shown in Eq. (24). In contrast to envelopes, all phases are independent even those related to the high correlated envelopes (r_1, r_2) and (r_3, r_4) which is expected for complex covariance matrices. Probability density function (PDF) of the generated Rayleigh fading envelopes and uniform distributed phases are coincides with the theoretical results as shown in Figs. 5 and 6, respectively. The results shown in Figs. 3–6 demonstrate the effectiveness of simulating the desired correlated fading signals with complex covariance matrices.

For comparison purpose, envelopes (r_1, r_2, r_3, r_4) and phases (β_1, β_2, β_3, β_4) of generated fading signals using Cholesky and eigenvalue based methods are depicted in Figs. 7 and 8, respectively. In these methods, the negative eigenvalue (-0.254) is replaced by small positive value ($\delta = 10^{-3}$) and zero for Cholesky and eigenvalue factorizations, respectively. In Table 4, the measured correlations of simulated fading envelopes are compared with the desired values. As can be seen, results of GSCT are very close to the desired values and outperform those of conventional methods which prove the accuracy of proposed technique. Note that in GSCT, correlations of nonsuccessive envelopes are approximated by the associated successive envelope correlations using Eq. (18) as $\rho_{13} = \rho_{24} = 0.223$ and $\rho_{14} = 0.2$. These values are in the admissible accuracy range of desired correlations and close to the measured results.

Example 2. In this example, we consider generation of $\mathcal{N} = 4$ equal power flat Rayleigh fading signals as $\mathbf{A} = [a_1 \quad a_2 \quad a_3 \quad a_4]$ for 4 receive antenna correlation scenario. The constant spatial correlation model [24] is adopted in this example due its popularity by using the following real constant receive covariance matrix reflecting small separation distance among antennas.

$$\mathbf{R}_{AA} = \begin{bmatrix} 1 & \gamma_{12} & \gamma_{13} & \gamma_{14} \\ \gamma_{21}^* & 1 & \gamma_{23} & \gamma_{24} \\ \gamma_{31}^* & \gamma_{32}^* & 1 & \gamma_{34} \\ \gamma_{41}^* & \gamma_{42}^* & \gamma_{43}^* & 1 \end{bmatrix} = \begin{bmatrix} 1 & 0.9 & 0.9 & 0.9 \\ 0.9 & 1 & 0.9 & 0.9 \\ 0.9 & 0.9 & 1 & 0.9 \\ 0.9 & 0.9 & 0.9 & 1 \end{bmatrix} \tag{26}$$

The eigenvalues of $\mathbf{R}_{AA}$ are: 0.061, 0.102, 0.309, and 3.526 . Since all eigenvalues are positive, $\mathbf{R}_{AA}$ is a positive definite matrix and many conventional methods such as Tran et al. [26], Sorooshyari and Daut [27], Natarajan et al. [30], Beaulieu and Merani [31], Baddour and Beaulieu [32], and Chung et al. [33] can be used to generate the desired fading signals with high level of accuracy.

Using Eq. (11) with $\sigma_a^2 = 2\ell = 1$, the desired correlation matrix of envelopes ρ can be calculated directly from $\mathbf{R}_{AA}$ as

$$\rho = \begin{bmatrix} 1 & \rho_{12} & \rho_{13} & \rho_{14} \\ \rho_{21} & 1 & \rho_{23} & \rho_{24} \\ \rho_{31} & \rho_{32} & 1 & \rho_{34} \\ \rho_{41} & \rho_{42} & \rho_{43} & 1 \end{bmatrix} = \begin{bmatrix} 1 & 0.81 & 0.81 & 0.81 \\ 0.81 & 1 & 0.81 & 0.81 \\ 0.81 & 0.81 & 1 & 0.81 \\ 0.81 & 0.81 & 0.81 & 1 \end{bmatrix} \tag{27}$$

Therefore, desired correlation vector ρ_s of successive envelopes is

$$\boldsymbol{\rho_s} = [\rho_{12} \quad \rho_{23} \quad \rho_{34}] = [0.81 \quad 0.81 \quad 0.81] \tag{28}$$

In this example, all propagation factors $\mathbb{k}_{kq}, (k \neq q) = 1, \ldots, 4$ are zero since $\mathbf{R}_{AA}$ is a real covariance matrix. Envelopes (r_1, r_2, r_3, r_4) and phases (β_1, β_2, β_3, β_4) of the generated fading signals are depicted in Figs. 9 and 10, respectively. As can be seen, all phases and envelopes are closely correlated as expected for the given real covariance matrices. In this case, the inphase and quadrature components of any two signals a_k and a_q are uncorrelated where $\mathrm{E}\{x_k y_q\} = -\mathrm{E}\{y_k x_q\} = 0$ in contrast to $\mathrm{E}\{x_k y_q\} = -\mathrm{E}\{y_k x_q\} = \mathbb{p}_{kq}$ when complex covariance matrices are used (see Example 1). This example demonstrates the

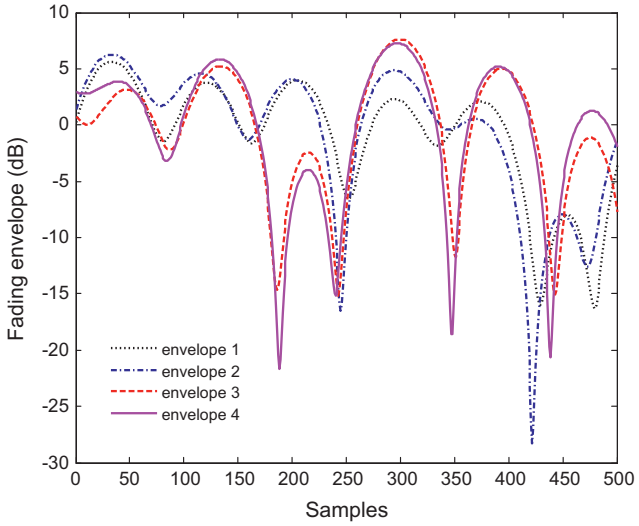

Fig. 3. Equal power envelopes of **A** generated using GSCT for the parameters given in Example 1 as; $\sigma_a^2 = 1, \rho_{12} = \rho_{34} = 0.89, \rho_{23} = 0.25, \mathbb{k}_{12} = \mathbb{k}_{34} = 1.29$, and $\mathbb{k}_{23} = 2.76$ which are related to complex $\mathbf{R}_{AA}$.

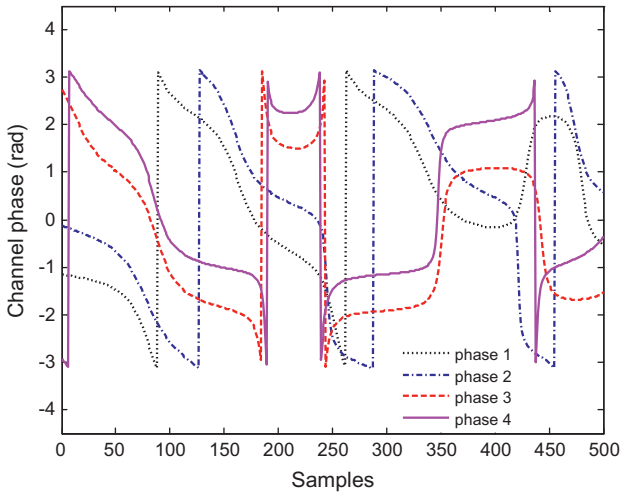

Fig. 4. Phases of equal power signals of **A** generated using GSCT for the parameters given in Example 1 as; $\sigma_a^2 = 1, \rho_{12} = \rho_{34} = 0.89, \rho_{23} = 0.25, \mathbb{k}_{12} = \mathbb{k}_{34} = 1.29$, and $\mathbb{k}_{23} = 2.76$ which are related to complex $\mathbf{R}_{AA}$.

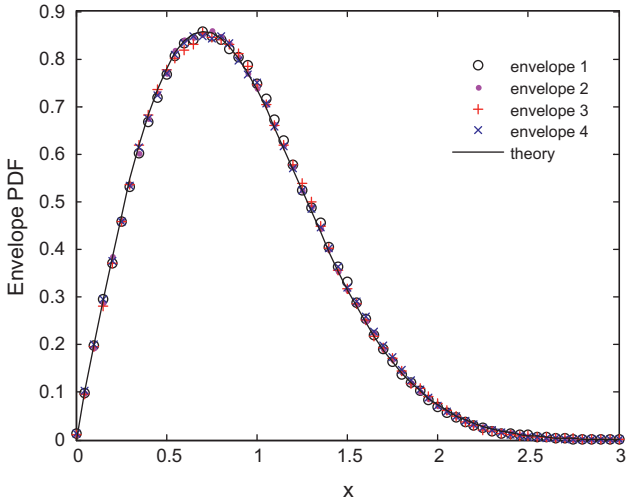

Fig. 5. PDF of the Rayleigh fading envelopes of **A** signals generated in Example 1.

applicability and accuracy of simulating signals with real covariance matrices using GSCT with less complexity compared with conventional methods.

Example 3. Channels of many communication systems include large number of spectrally correlated fading signals. In this example, we consider generation of $\mathcal{N} = 64$ equal power correlated flat Rayleigh fading signals as $\mathbf{A} = [a_1 \quad a_2 \quad \cdots \quad a_{64}]$ for multi-carrier system scenario of 64 subcarriers. Based on IEEE 802.11a specifications (OFDM) [4,27], the following parameters are adopted in this example as: frequency separation between adjacent frequencies of $\Delta f = 312.5$ kHz, channel delay spread $\sigma_\tau = 0.1$ μs, maximum Doppler frequency $f_d = 50$ Hz, arrival time delay between any adjacent signals are $\tau_{(k-1)k} = 1$ ms, $k = 1, \ldots, 64$, and power of each signal is $\sigma_a^2 = 2\ell = 1$.

Using Eqs. (5), (6), and (11), the desired correlation vector ρ_s of successive envelopes can be calculated from the given parameters as

$$\boldsymbol{\rho_s} = \left[\rho_{12} \quad \rho_{23} \quad \cdots \quad \rho_{(63)(64)}\right] = [0.91 \quad 0.91 \quad \cdots \quad 0.91] \tag{29}$$

where the calculated propagation factors are $\mathbb{k}_{(k-1)k} = 0.196, k = 1, \ldots, 64$.

From the generated signal of **A** using GSCT, envelopes r_1, r_2, r_3, and r_{64} are shown only in Fig. 11 for simplicity. As can be seen, frequency separation between signals is one of the parameters that has great impact on the channel correlation where as Δf decreased, the correlation increased. For example, envelopes r_1, r_2, and r_3 are highly correlated while r_3 appears

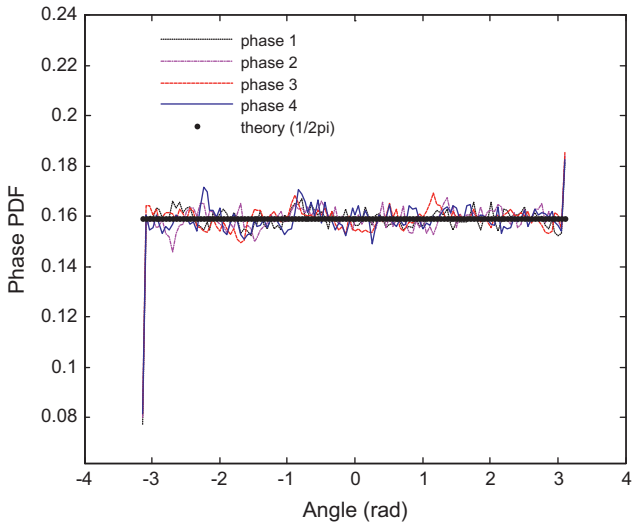

Fig. 6. PDF of uniform distribution phases of **A** signals generated in Example 1.

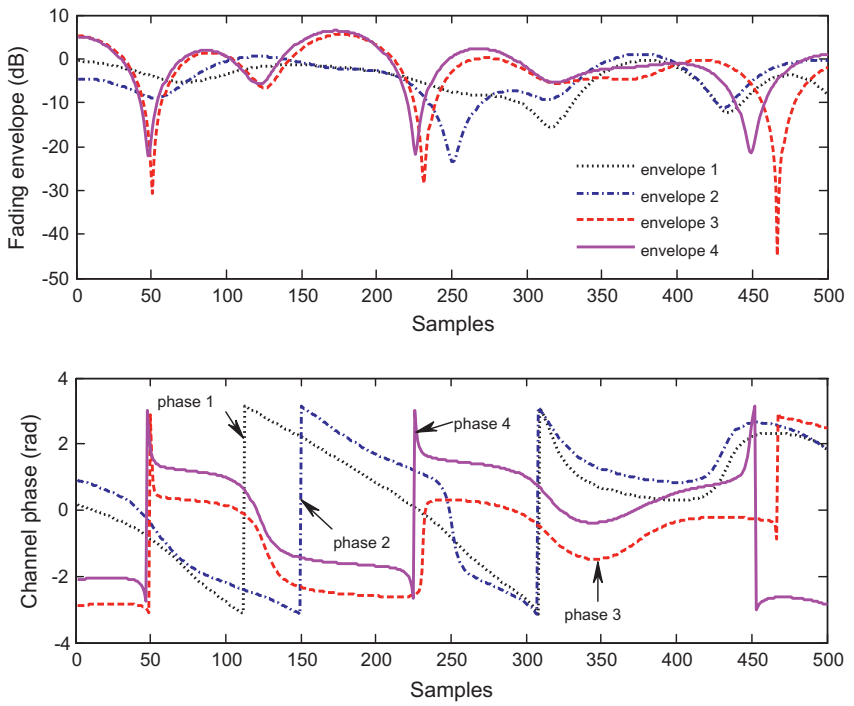

Fig. 7. Equal power envelopes and phases of **A** generated using Cholesky decomposition based method [27] for the parameters given in Example 1 as; $\sigma_a^2 = 1, \rho_{12} = \rho_{34} = 0.89, \rho_{23} = 0.25, \mathbb{k}_{12} = \mathbb{k}_{34} = 1.29$, and $\mathbb{k}_{23} = 2.76$ which are related to complex $\mathbf{R}_{AA}$.

independent to them. The measured correlations for these envelopes are; $\rho_{12} = 0.91$, $\rho_{23} = 0.91$, $\rho_{13} = 0.82$, and $\rho_{1(64)} = \rho_{2(64)} = \rho_{3(64)} \cong 0.0$. It should be noted that none of the existing methods can generate the desired signals of this example due to the large number of signals.

Example 4. In many applications of wireless communication systems such as MC-CDMA, MU-MIMO, and MIMO–OFDM, the fading channel exhibits unequal power signals due to system design requirement or inaccurate power control. In such systems, spectral and/or spatial correlation may occur frequently. Therefore, we consider generation of $\mathcal{N} = 4$ correlated flat Rayleigh fading signals in this example as $\widehat{\mathbf{A}} = \begin{bmatrix} \hat{a}_1 & \hat{a}_2 & \hat{a}_3 & \hat{a}_4 \end{bmatrix}$ for unequal power scenario using the following setting:

Signal power: $\sigma_{\hat{a}_1}^2 = \sigma_{\hat{a}_2}^2 = 1, \sigma_{\hat{a}_3}^2 = 2$, and $\sigma_{\hat{a}_4}^2 = 3$.

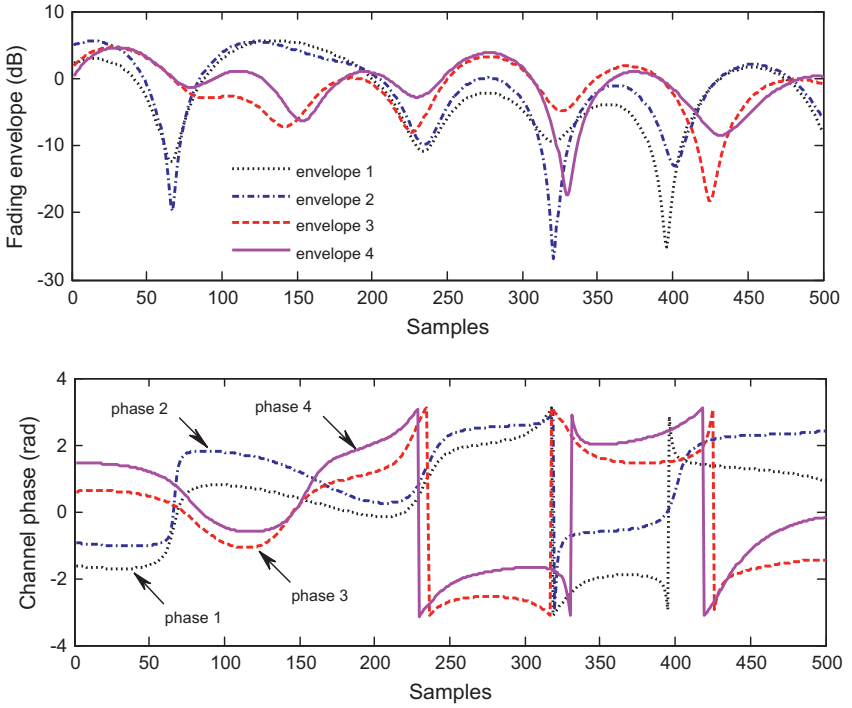

Fig. 8. Equal power envelopes and phases of **A** generated using eigenvalue decomposition based method [26] for the parameters given in Example 1 as; $\sigma_a^2 = 1, \rho_{12} = \rho_{34} = 0.89, \rho_{23} = 0.25, \mathbb{k}_{12} = \mathbb{k}_{34} = 1.29$, and $\mathbb{k}_{23} = 2.76$ which are related to complex $\mathbf{R}_{AA}$.

Table 4
Measured correlations of equal power correlated fading signal envelopes generated using GSCT, Cholesky decomposition based method [27], and eigenvalue decomposition based method [26] compared with the desired values of Example 1.

Correlation	ρ_{12}	ρ_{23}	ρ_{34}	ρ_{13}	ρ_{24}	ρ_{14}
Desired	0.898	0.249	0.898	0.215	0.207	0.225
Measured (GSCT)	0.897	0.250	0.902	0.221	0.201	0.224
Measured (Cholesky)	0.873	0.224	0.882	0.237	0.218	0.207
Measured (eigenvalue)	0.921	0.262	0.911	0.233	0.213	0.211

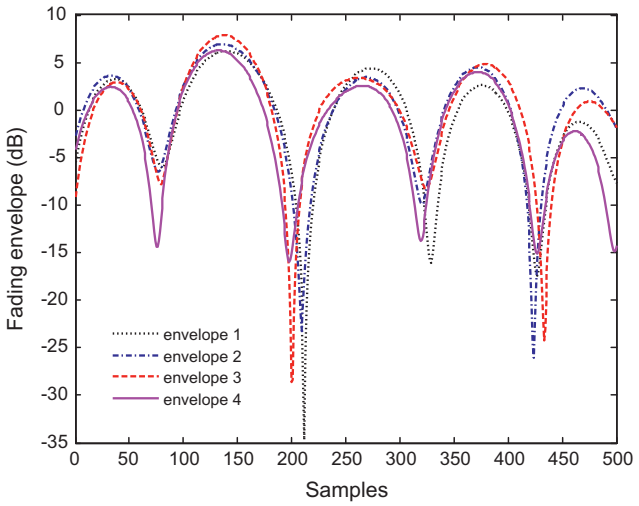

Fig. 9. Equal power envelopes of **A** generated using GSCT for the parameters given in Example 2 as; $\sigma_a^2 = 1, \rho_{12} = \rho_{23} = \rho_{34} = 0.81$ and $\mathbb{k}_{12} = \mathrm{k}_{23} = \mathbb{k}_{34} = 0.0$ which are related to real $\mathbf{R}_{AA}$.

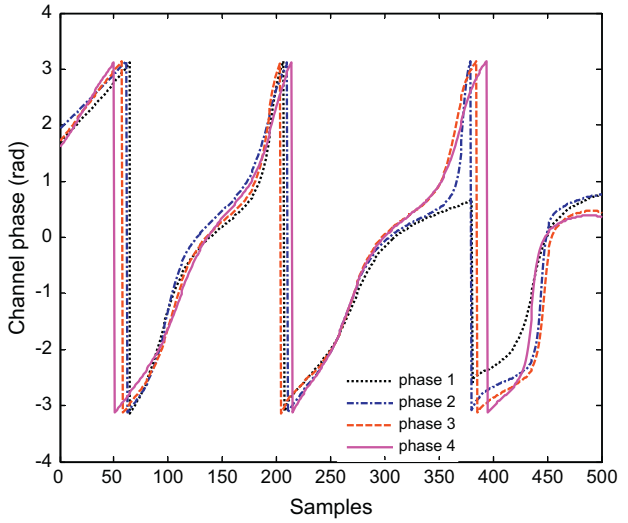

Fig. 10. Phases of equal power signals of **A** generated using GSCT for the parameters given in Example 2 as; $\sigma_a^2 = 1, \rho_{12} = \rho_{23} = \rho_{34} = 0.81$ and $\mathbb{k}_{12} = \mathbb{k}_{23} = \mathbb{k}_{34} = 0.0$ which are related to real $\mathbf{R}_{AA}$.

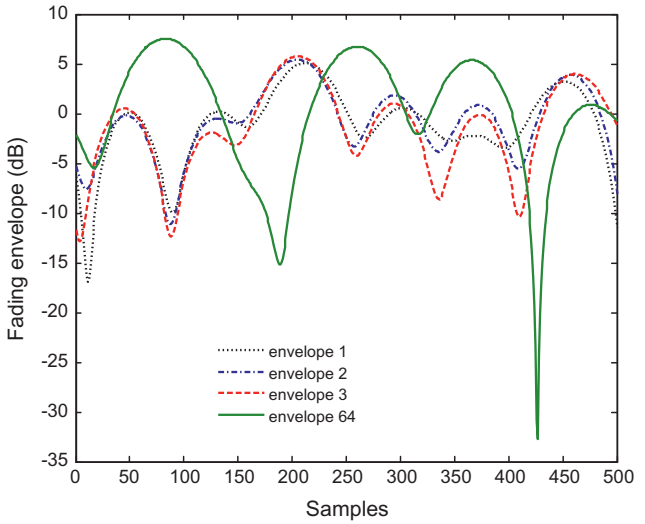

Fig. 11. Equal power envelopes of **A** generated using GSCT for the parameters given in Example 3 as; $\sigma_a^2 = 1, \rho_{12} = \rho_{23} = \rho_{(63)(64)} = 0.91$ and $\mathbb{k}_{(k-1)k} = 0.196, k = 1, \ldots, 64$.

Propagation factors: $\mathbb{k}_{12} = \mathbb{k}_{23} = \mathbb{k}_{34} = 1$.
Desired correlation vector $\hat{\boldsymbol{\rho}}_{\boldsymbol{s}}$ of successive envelopes is

$$\hat{\boldsymbol{\rho}}_{\boldsymbol{s}} = [\,\hat{\rho}_{12} \quad \hat{\rho}_{23} \quad \hat{\rho}_{34}\,] = [\,0.9 \quad 0.3 \quad 0.7\,] \tag{30}$$

Using GSCT, the first step involves generation of equal unit power correlated Rayleigh fading signals $\mathbf{A} = [\,a_1 \quad a_2 \quad a_3 \quad a_4\,]$ with normalized correlation vector ρ_s calculated from $\hat{\boldsymbol{\rho}}_{\boldsymbol{s}}$ using Eq. (21) as

$$\boldsymbol{\rho}_{\boldsymbol{s}} = [\,\rho_{12} \quad \rho_{23} \quad \rho_{34}\,] = [\,0.9 \quad 0.21 \quad 0.28\,] \tag{31}$$

In Fig. 12, envelopes (r_1, r_2, r_3, r_4) of the generated signals **A** are shown which reflects the correlation values of ρ_s while all phases (β_1, β_2, β_3, β_4) are independent since the corresponding covariance matrix of these signals is complex. In the second step, desired unequal power signals $\widehat{\mathbf{A}}$ are calculated from **A** using Eq. (22). Unequal power envelopes $(\hat{r}_1, \hat{r}_2, \hat{r}_3, \hat{r}_4)$ of $\widehat{\mathbf{A}}$ are depicted in Fig. 13 reflecting the desired signal power and correlations of $\hat{\boldsymbol{\rho}}_{\boldsymbol{s}}$ while all phases $(\hat{\beta}_1, \hat{\beta}_2, \hat{\beta}_3, \hat{\beta}_4)$ are independent as in the first step. From these figures, it can be seen that envelopes r_3 and r_4 are differ than $\hat{r}_3$ and $\hat{r}_4$ due to the power

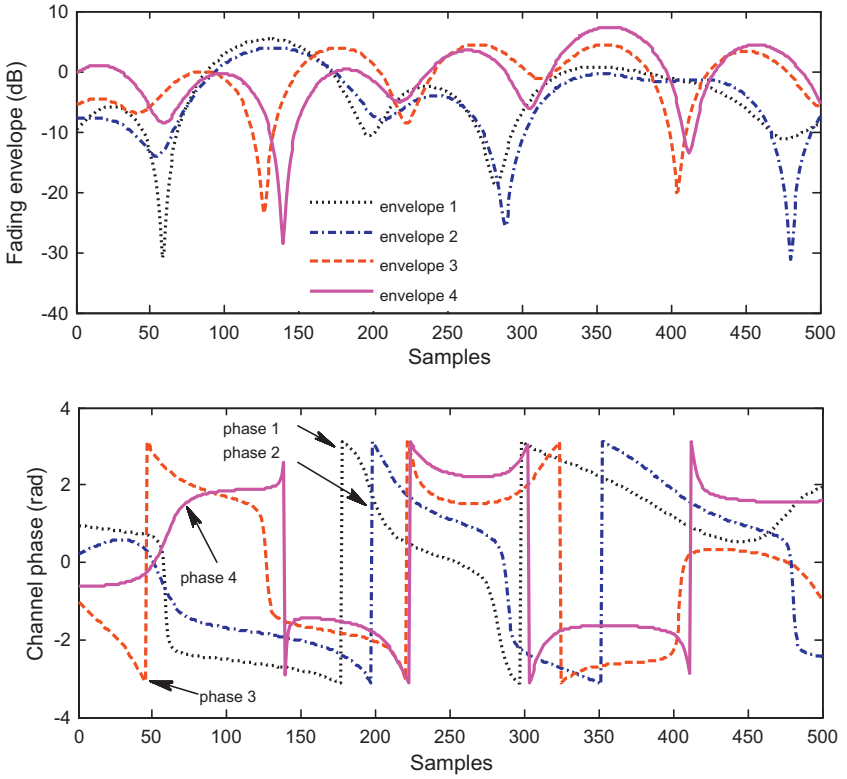

Fig. 12. Equal unit power envelopes $\left(\sigma^2_{a_1} = \sigma^2_{a_2} = \sigma^2_{a_3} = \sigma^2_{a_4} = 1\right)$ and phases of **A** generated in the first step of GSCT for the parameters calculated in Example 4 as; $\rho_{12} = 0.9$, $\rho_{23} = 0.21$, and $\rho_{34} = 0.28$.

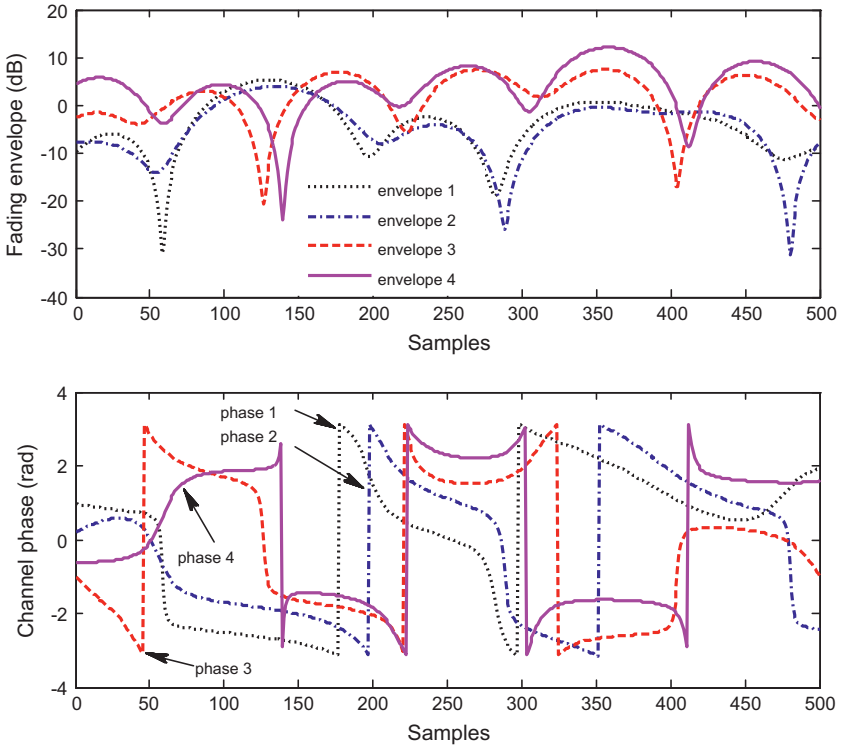

Fig. 13. Unequal power envelopes and phases of desired $\widehat{\mathbf{A}}$ generated in the second step of GSCT for the parameters given in Example 4 as; $\sigma^2_{a_1} = \sigma^2_{a_2} = 1, \sigma^2_{a_3} = 2, \sigma^2_{a_4} = 3, \hat{\rho}_{12} = 0.9, \hat{\rho}_{23} = 0.3, \hat{\rho}_{34} = 0.7$, and $\mathbb{k}_{12} = \mathbb{k}_{23} = \mathbb{k}_{34} = 1$.

difference in first and second steps of generation while r_1 and r_2 are same as $\hat{r}_1$ and $\hat{r}_2$ since they have equal powers in both steps. On the other hand, all phases in the first step are similar to that of second step and not affected by the power transformation as expected. Results of this example demonstrate the applicability of designing unequal power correlated fading signals using GSCT.

7. Conclusions

In this paper, GSCT technique is proposed for the accurate generation of equal/unequal power correlated Rayleigh fading channels for multi-antenna and multicarrier systems where spatial and spectral correlations are very common. It employs real correlation vector of successive signal envelopes to avoid the high computational complexity burden for covariance matrix decomposition required in conventional methods. In contrast to existing techniques, any number of fading signals with any desired correlations of successive envelopes can be generated accurately using GSCT as demonstrated by simulations of different practical system scenarios. It overcomes all shortcomings of conventional methods particularly as the number of fading signals increased and/or moderate to high correlations is used. For small number of fading signals and/or low correlation levels where the existing methods can be applied, GSCT provides similar high accuracy results for the successive signals with significant reduction in computational complexity. The simplicity and accuracy of this technique will help the researchers and engineers to study and simulate the impact of channel correlations on the existing and new wireless communication schemes.

References

[1] J. Mietzner, R. Schober, L. Lampe, W. Gerstacker, A. Hoeher, Multiple-Antenna techniques for wireless communications – a comprehensive literature survey, IEEE Commun. Surveys Tutorials 11 (2) (2009) 87–105.
[2] A. Paulraj, D. Gore, R. Nabar, H. Bolcskei, An overview of MIMO communications – a key to gigabit wireless, IEEE Proc. 92 (2) (2004) 198–218.
[3] D. Gesbert, M. Kountouris, R.W. Heath Jr., C. CHae, T. Salzer, From single-user to multiuser communications: shifting the MIMO paradigm, IEEE Signal Process. Mag. 24 (5) (2007) 36–46.
[4] N. Jaber, K.E. Tepe, E. Abdel-Raheem, Reconfigurable simulator using graphical user interface (GUI) and object-oriented design for OFDM systems, Simul. Model. Practice Theory 19 (2011) 1294–1317.
[5] F. Zabini, B. Masini, A. Conti, L. Hanzo, Partial equalization for MC-CDMA systems in non-ideally estimated correlated fading, IEEE Trans. Vehicular Technol. 59 (8) (2010) 3818–3830.
[6] M. Jiang, L. Hanzo, Multiuser MIMO–OFDM for next-generation wireless systems, IEEE Proc. 95 (7) (2007) 1430–1469.
[7] H. Huang, H. Viswanathan, G. Foschini, Multiple antennas in cellular CDMA systems: transmission, detection, and spectral efficiency, IEEE Trans. Wireless Commun. 1 (3) (2002) 383–392.
[8] L.L. Yang, MIMO-assisted space-code-division multiple-access: linear detectors and performance over multipath fading channels, IEEE J. Sel. Areas Commun. 24 (1) (2006) 121–131.
[9] M. Juntti, M. Vehkapera, J. Leinonen, Z. Li, D. Tujkovic, MIMO MC-CDMA communications for future cellular systems, IEEE Commun. Mag. 43 (2) (2005) 118–124.
[10] Y. Zhang, J. Zhang, P. Smith, M. Shafi, P. Zhang, Reduced complexity channel models for IMT-advanced evaluation, EURASIP J. Wireless Commun. Netw. 1 (2009) 1–13.
[11] P. Almers, E. Bonek, A. Burr, N. Czink, M. Debbah, et al, Survey of channel and radio propagation models for wireless MIMO systems, EURASIP J. Wireless Commun. Netw. 1 (2007) 1–19.
[12] W. Xu, S. Zekavat, H. Tong, A novel spatially correlated multiuser MIMO channel modeling: impact of surface roughness, IEEE Trans. Anten. Propag. 57 (8) (2009) 2429–2438.
[13] A. Abdi, M. Kaveh, A space-time correlation model for multielement antenna systems in mobile fading channels, IEEE J. Sel. Areas Commun. 20 (3) (2002) 550–560.
[14] R. Ertel, P. Cardieri, K. Sowerby, T. Rappaport, J. Reed, Overview of spatial channel models for antenna array communication systems, IEEE Pers. Commun. Mag. 5 (1) (1998) 10–22.
[15] B. SKLAR, Rayleigh fading channels in mobile digital communication systems, part I: characterization, IEEE Commun. Mag. 35 (7) (1997) 90–100.
[16] B. SKLAR, Rayleigh fading channels in mobile digital communication systems, part II: mitigation, IEEE Commun. Mag. 35 (7) (1997) 102–109.
[17] W.C. Jakes, Microwave Mobile Communications, Wiley, New York, 1974.
[18] R. Clarke, A statistical theory of mobile-radio reception, Bell Syst. Tech. J. (1968) 957–1000.
[19] Y. Zheng, C. Xiao, Improved models for the generation of multiple uncorrelated Rayleigh fading waveforms, IEEE Commun. Lett. 6 (6) (2002) 256–258.
[20] C.-X. Wang, M. Patzold, D. Yuan, Accurate and efficient simulation of multiple uncorrelated Rayleigh fading waveforms, IEEE Trans. Wireless Commun. 6 (3) (2007) 833–839.
[21] L. Hanzo, M. Munster, B. Choi, T. Keller, OFDM and MC-CDMA for Broadband Multiuser Communications, WLANs and Broadcasting, IEEE Press/Wiley, Piscataway, NJ, 2003.
[22] H. Bolcskei, D. Gesbert, A. Paulraj, On the capacity of OFDM-BASED spatial multiplexing systems, IEEE Trans. Commun. 50 (2) (2002) 225–234.
[23] M. Kang, M.S. Alouini, Capacity of correlated MIMO Rayleigh channels, IEEE Trans. Wireless Commun. 5 (1) (2006) 143–155.
[24] H. Shin, J. Lee, Capacity of multiple-antenna fading channels: spatial fading correlation, double scattering, and keyhole, IEEE Trans. Inform. Theory 49 (10) (2003) 2636–2647.
[25] C-N. Chuah, D. Tse, J. Khan, R. Valenzuela, Capacity scaling in MIMO wireless systems under correlated fading, IEEE Trans. Inform. Theory 48 (3) (2002) 637–650.
[26] L. Tran, T. Wysocki, A. Mertins, J. Seberry, A generalized algorithm for the generation of correlated Rayleigh fading envelopes in wireless channels, EURASIP J. Wireless Commun. Netw. 5 (2005) 801–815.
[27] S. Sorooshyari, D. Daut, On the generation of correlated Rayleigh fading envelopes for accurate simulation of diversity channels, IEEE Trans. Commun. 54 (8) (2006) 1381–1386.
[28] R. Ertel, J. Reed, Generation of two equal power correlated Rayleigh fading envelopes, IEEE Commun. Lett. 2 (10) (1998) 276–278.
[29] N. Beaulieu, Generation of correlated Rayleigh fading envelopes, IEEE Commun. Lett. 3 (6) (1999) 172–174.
[30] B. Natarajan, C. Nassar, V. Chandrasekhar, Generation of correlated Rayleigh fading envelopes for spread spectrum applications, IEEE Commun. Lett. 4 (1) (2000) 9–11.

[31] N. Beaulieu, M. Merani, Generation of multiple Rayleigh fading sequences with specified cross-correlations, Eur. Trans. Telecommun. 15 (2004) 471–476.
[32] K. Baddour, N. Beaulieu, Accurate simulation of multiple cross-correlated Rician fading channels, IEEE Trans. Commun. 52 (11) (2004) 1980–1987.
[33] W.-H. Chung, R. Hudson, K. Yao, A unified approach for generating cross-correlated and auto-correlated MIMO fading envelope processes, IEEE Trans. Commun. 57 (11) (2009) 3481–3488.
[34] D. Young, N. Beaulieu, The generation of correlated Rayleigh random variates by inverse discrete Fourier transform, IEEE Trans. Commun. 48 (7) (2000) 1114–1127.
[35] C.-X. Wang, D. Yuan, H.-H. Chen, W. Xu, An improved deterministic SoS channel simulator for multiple uncorrelated Rayleigh fading channels, IEEE Trans. Wireless Commun. 7 (9) (2008) 3307–3311.